Astron. Astrophys. 344, 755–766 (1999)

ASTRONOMY AND ASTROPHYSICS

X-ray study of the NGC 383 group of galaxies and the source 1E 0104+3153

Stefanie Komossa and Hans Böhringer

Max-Planck-Institut für Extraterrestrische Physik, Postfach 1603, D-85740 Garching, Germany

Received 19 October 1998 / Accepted 11 January 1999

Abstract. We present results from an analysis of the X-ray properties of the NGC 383 galaxy group based on *ROSAT* PSPC and HRI data. X-ray emission can be traced out to $\sim 1 h_{50}^{-1}$ Mpc, the estimated virial radius of the system. We determine a total mass of $6\,10^{13} h_{50}^{-1}$ $M_\odot$ for the group inside this radius with a gas mass fraction of 21%. The intragroup gas temperature of 1.5 keV is both consistent with the galaxy velocity dispersion and the X-ray luminosity – temperature relation of groups and clusters suggesting that the group is fairly relaxed. This is also indicated by the almost spherically symmetric appearance of the group's X-ray halo.

The X-ray properties of the radio galaxy NGC 383 (3C 31) which is located near the center of the group are discussed. Its spectrum is best described by a two-component model, consisting of emission from a low-temperature Raymond-Smith plasma, and a hard tail. The emission from NGC 383 is not resolved by the *ROSAT* HRI. The possible interaction of the radio jets of 3C 31 with the IGM is studied.

A spatial, spectral and temporal analysis of the *Einstein* source 1E0104+3153 located within the field of view is performed, one goal being the identification of the optical counterpart (with both, a high-redshift BAL quasar and a nearby elliptical galaxy, member of a small group, located within the *Einstein* X-ray error circle). We find evidence that the IGM of the small group contributes significantly to the X-ray emission of 1E0104, which can be described by a Raymond-Smith model of $kT \simeq 2$ keV and a soft X-ray luminosity of $L_{\rm x} \simeq 3\,10^{43}$ erg/s.

Key words: cosmology: dark matter – galaxies: clusters: individual: NGC 383 group – galaxies: individual: NGC 383 = 3C31, 1E0104+3153 – galaxies: elliptical and lenticular, cD – X-rays: galaxies

1. Introduction

NGC 383, of type S0 (Arp 1968), is a member of a bright chain of galaxies (Arp 1966, Arp & Bertola 1971, Kormendy & Bahcall 1974), which itself belongs to a group of galaxies (Zwicky et al. 1961) located within the Perseus-Pisces filament. NGC 383 is at redshift z=0.017 and has a companion galaxy in 33″ distance.

Send offprint requests to: St. Komossa (skomossa@xray.mpe.mpg.de)

NGC 383 is a moderately bright radio galaxy (3C 31) and has been extensively studied at radio wavelengths in the past (e.g., Macdonald et al. 1968, Burch 1977,1979, Klein & Wielebinski 1979, Fomalont et al. 1980, Ekers et al. 1981, van Breugel 1982, Strom et al. 1983, Condon et al. 1991, Andernach et al. 1992, Artyukh et al. 1994, Lara et al. 1997, Henkel et al. 1998). It shows a symmetric edge darkened double-source structure with two strong jets. The origin of the structures seen in the radio morphology of dominant cluster/group members is still not well understood. The structures of the jets of NGC 383 were interpreted by Blandford & Icke (1978) as due to tidal interaction with the companion galaxy NGC 382. However, Fraix-Burnet et al. (1991) found no evidence for interaction between the two galaxies. Further jet models were presented by Bridle et al. (1980) and Bicknell (1984). Whereas Butcher et al. (1980) reported evidence for a detection of the jet at optical wavelengths, this was not confirmed by later studies (Keel 1988, Owen et al. 1990, Fraix-Burnet et al. 1991).

The optical spectrum of the nucleus is characterized by emission lines. The optical emission was found to be extended, and in form of a rotating disk (Owen et al. 1990) or ring (Fraix-Burnet et al. 1991) that coincides with a dust-ring reported by Butcher et al. (1980). The emission line ratios in the disk were found to be similar to those at the nucleus and Owen et al. concluded that the disk ionization is probably driven by the nucleus.

NGC 383 is the brightest member of a rich group of galaxies. The group is included in the Zwicky catalogue; membership studies based on velocity measurements were performed by Moss & Dickens (1977), Garcia (1993), Sakai et al. (1994), and Ledlow et al. (1996), who included 25, 22, 16, 32 member galaxies, respectively. Among the 27 groups studied, Ledlow et al. found the galaxy velocity distribution to significantly deviate from a Gaussian in 55% of them; the NGC 383 group was not among those. Sakai et al., using a standard estimator as in Heisler et al. (1985), derived a virial mass of $M_{\rm vir}$ = $0.2\,10^{14}$ $hM_\odot$, and a mass-light ratio M/L = 240. Extended X-ray emission from the group was first detected by *Einstein* (Fabbiano et al. 1984). The data were analyzed by Morganti et al. (1988) in the course of a large sample study of the effect of gas pressure on radio sources.

To perform a detailed spatial and spectral analysis of the X-ray emission from NGC 383, the intra-group medium (IGM),

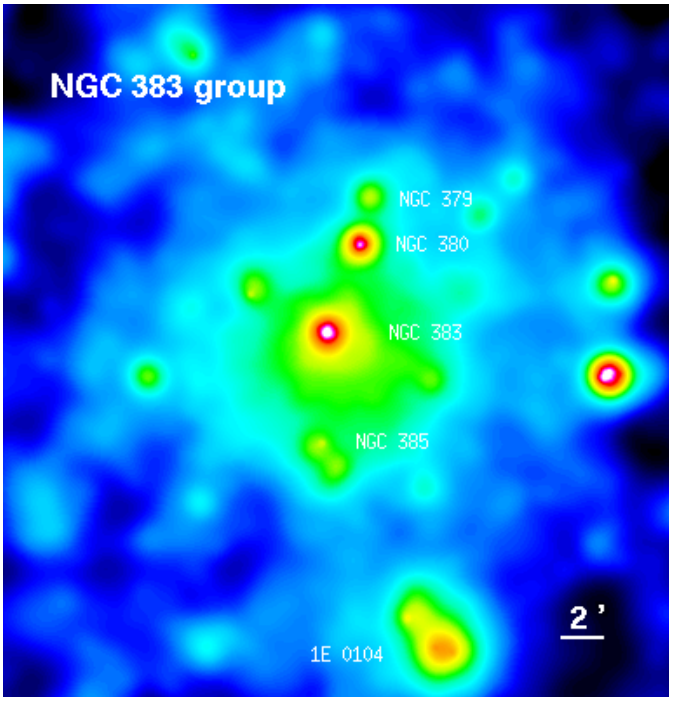

Fig. 1. *ROSAT* PSPC X-ray image of the central region of the NGC 383 group of galaxies. The image was smoothed with a variable Gaussian filter of widths σ = 1′, 0.5′, 20″, 7.5″, 5″ and 3.5″. Several galaxies of the optical chain Arp 331, and the *Einstein* source 1E 0104+3153 are marked. Note the detection of another X-ray source close to 1E 0104.

and an investigation of the relation with the radio jet, a *ROSAT* PSPC observation was applied for. These data presented here have been previously partly analyzed by Trussoni et al. (1997; T97 hereafter) in a study of hot coronae in nearby radio galaxies. Here, we extent their analysis and focus on the properties of the IGM and the NGC 383 group as a whole, in particular, the determination of gas and total mass; and the nature of the X-ray emission from NGC 383. We also briefly discuss new HRI data which were retrieved from the archive.

Also located in the field of view is the high-redshift (z=2.027) BAL quasar QSO 0104+3153. X-ray emission from the direction of this quasar was discovered in the *Einstein* Medium Sensitivity Survey (Stocke et al. 1984). The QSO, and a nearby (10″) giant elliptical galaxy, member of a small group, were identified as possible counterparts of the X-ray emission. Due to its proximity to the elliptical, the quasar is considered as prime candidate for lensing by halo stars. Optical variability of $\sim 0.5^{\rm m}$ was detected by Gioia et al. (1986). The *ROSAT* PSPC spectrum was briefly discussed in a large sample study by Ciliegi & Maccacaro (1996). The identification of the source (QSO, elliptical galaxy or IGM of the small group) remained unclear. Here, we perform a detailed study of the properties of this X-ray source and address the counterpart question on the basis of (i) long- and short-term variability behaviour, (ii) X-ray spectral shape, (iii) improved spatial position obtained with the HRI.

Physical parameters are calculated for $H_{\rm o}$ = 50 km/s/Mpc, $q_{\rm o}$ = 0.5 and assuming the galaxies/group to follow the Hubble flow. For the distance of the NGC 383 group, 1″ corresponds to a scale of 0.5 kpc.

2. X-ray data

2.1. PSPC

The group was the target of a pointed *ROSAT* PSPC (Trümper 1983; Pfeffermann et al. 1987) observation with NGC 383 in the center of the field of view. Our observation was performed from July 28–29, 1991 with a duration of 27.5 ksec. The satellite was not in wobble mode during this observation.

The background was usually determined in a source-free ring around the target source (for details see below). The data were corrected for vignetting and dead-time, using the EXSAS software package (Zimmermann et al. 1994). Widely extended X-ray emission is present (Fig. 1). The central region appears roughly circularly symmetric. Emission from the group can be traced out to a distance of $\sim$33′ radius ($\sim$ 1 Mpc). The total countrate (channels 52–201) within this region is 0.58 $\pm$0.01 cts/s. Several group ellipticals are individually detected, the brightest with countrates of 0.024$\pm$0.001 cts/s (NGC 383), 0.0058$\pm$0.0006 cts/s (NGC 379), 0.0124$\pm$0.0008 cts/s (NGC 380), 0.0041$\pm$0.0005 cts/s (NGC 385), and 0.0021$\pm$0.0006 cts/s (NGC 384) as summarized in Table 2. X-ray emission from the direction of 1E 0104 is detected with 0.028$\pm$0.001 cts/s.

To carry out the spectral analysis of the individual sources, photons in the amplitude channels 11–240 were binned according to a constant signal/noise ratio of $\geq 5\sigma$.

Results given below refer to the PSPC data if not mentioned otherwise.

2.2. HRI

An HRI observation centered on NGC 383 was performed between July 11 and 25, 1994 with a duration of 25.0 ksec. The data were retrieved from the archive. (An earlier HRI observation, of Jan. 1992 with 2.8 ksec duration, is briefly discussed in T97.) Due to the lower sensitivity of the HRI, essentially only the bright point-like sources are detected. These data are analyzed mainly to study the spatial structure of the X-ray emission from the bright group galaxies, and to search for variability in individual sources.

3. Group analysis

3.1. Spectral properties

A Raymond-Smith (rs) model was fit to the extended X-ray emission. If not noted otherwise, abundances were fixed to 0.35$\times$solar (Anders & Grevesse 1989). In a first step, the group photons within a circular region of radius 1000″ were selected; in a second step, this region was split into an inner circle (radius 200″), an intermediate ring (200″ out to 500″) and an outer

ring (500″ to 1000″). Point-like sources were removed. To this end, we first carried out a source detection using the EXSAS software. This resulted in about 35 sources detected within the total field of view. For the brightest sources, extents were then determined by inspecting the radial source profiles (the radius where the source profile merges with the local background taken as source extent) and by comparison with the profile expected from the PSF of the detector (for a more detailed discussion of NGC 383 see Sect. 4.1.2). This resulted in source extraction radii of ∼100″ for the brightest central sources. The detected sources were then removed within circular regions centered on their X-ray positions. As background we selected a source-free circular region in the outer part of the fov. Since the spectrum below 0.5 keV is strongly dominated by background, we usually excluded photons below this energy from the spectral fit. Treating the cold absorption as free parameter always resulted in a value (nearly) consistent with the Galactic absorption towards NGC 383 ($N_{\rm gal} = 0.523\,10^{21}$ cm^{-3}, Dickey & Lockman 1990) within the errors. We therefore fixed $N_{\rm H} = N_{\rm gal}$.

For the total emission within 1000″ we find a temperature kT = 1.5±0.1 keV. The temperature values derived for the three separate regions are consistent with this value and with each other within the errors (Table 1). This value of T is somewhat lower than the one given in Morganti et al. (1988; their Table 2) on the basis of an *Einstein* IPC observation; they estimate $kT \approx$ 3 keV. To check the robustness of the obtained temperature, we performed a few tests: If we do *not* remove the point sources and re-fit the total spectrum we get kT = 1.4±0.1 keV; if we fit a thermal bremsstrahlung model we obtain kT = 1.4±0.2 keV; if an rs plasma with solar instead of depleted abundances is assumed, the quality of the fit slightly improves without affecting the value of the temperature within the errors and we derive kT = 1.6±0.1 keV. T97 obtain kT = 1.5 keV for abundances of 0.35×solar. Results of our spectral fits are summarized in Table 1.

Using kT = 1.5 keV and $N_{\rm H} = N_{\rm gal}$, the total (0.1–2.4 keV) luminosity within 33′ is $L_{\rm x} = 1.5\,10^{43}$ erg/s (= $1.3\,10^{43}$ erg/s if the abundances are fixed to the solar value).

3.2. Spatial analysis

All bright ellipticals of the optical chain Arp 331 are individually detected in X-rays. The center of the X-ray emission maximum from NGC 383 at α = 1$^{\rm h}$7$^{\rm m}$25.9, δ = 32°24′44.″5 (J 2000) coincides well with the position of the optical nucleus at α = 1$^{\rm h}$7$^{\rm m}$25.0, δ = 32°24′44.″8. For an overlay of the PSPC X-ray contours on an optical image of the NGC 383 group see T97 (their Fig. 1).

To derive physical properties of the group, we first assume spherical symmetry of the extended X-ray emission, the emission to be centered on NGC 383, and rough isothermality to hold. For critical comments on and justification of 'standard' assumptions see, e.g., Böhringer et al. 1998 (their Sects. 2, 3). A β-model (e.g., Cavaliere & Fusco-Femiano 1976, Gorenstein et al. 1978, Jones & Forman 1984) of the form

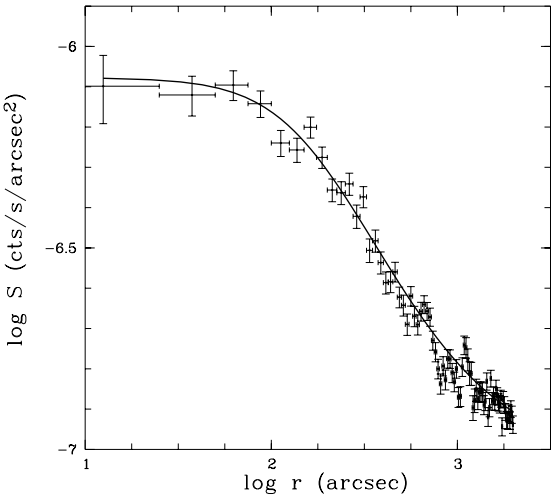

Fig. 2. Observed X-ray surface brightness profile (crosses) of the NGC 383 group of galaxies and best-fit β-modell (solid line). Due to the large extent of the emission, the data have not been PSF-convolved (a test with a fit of a convolved model did not show a significant change). Channels 52–201 were used to derive the surface brightness profile.

$$S = S_0(1 + \frac{r^2}{r_{\rm c}^2})^{-3\beta+\frac{1}{2}} \qquad (1)$$

was fit to the azimuthally averaged surface brightness profile of the PSPC observation (detected point sources were, again, removed except emission from NGC 383, inner bins were then excluded from the fit since they are dominated by emission from NGC 383 itself). This yields a central surface brightness $S_0 = 2.79\,10^{-3}$ cts/s/arcmin^2, a slope parameter β = 0.34 and a core radius $r_{\rm c}$ = 64 kpc. The gas mass enclosed inside 1 Mpc amounts to $M_{\rm gas}$ = $1.5\,10^{13}$ M$_\odot$. Inspection of Fig. 1 shows that NGC 383 is not located perfectly in the center of the large scale X-ray emission, but offset by about 1′ to the North-East. In fact, using the best-fit beta-model to construct a synthetic model image and subtracting the model image from the observed one leaves some residual extended emission to the SW and some 'negative' emission levels to the NE.

Therefore, in a second step, the surface brightness profile was centered at α = 1$^{\rm h}$7$^{\rm m}$22.8, δ = 32°23′45.″7 and re-fit after emission from NGC 383 was removed within a segment. In this case, we obtain $S_0 = 2.67\,10^{-3}$ cts/s/arcmin^2, $\beta = 0.38\pm0.03$, and $r_{\rm c} = 73^{+18}_{-15}$ kpc (errors are 1σ). The only slight change of the fit parameters underlines the robustness of the fit. The beta-model fit to the surface brightness profile is shown in Fig. 2. Again constructing a model image and subtracting this from the observed one now does not show any residual emission except the point-like sources. This model is also used for the gas and total mass estimate below.

These results differ from the previous analysis of T97 in yielding a smaller core radius (they derived $r_{\rm c}$ = 230 kpc) and shallower slope (they found β = 0.6) for the data presented here. We have checked that our results are robust (β varying between ∼ 0.3 and 0.45 in extreme cases) against non-removal of individual sources (up to all), shifts of the central position,

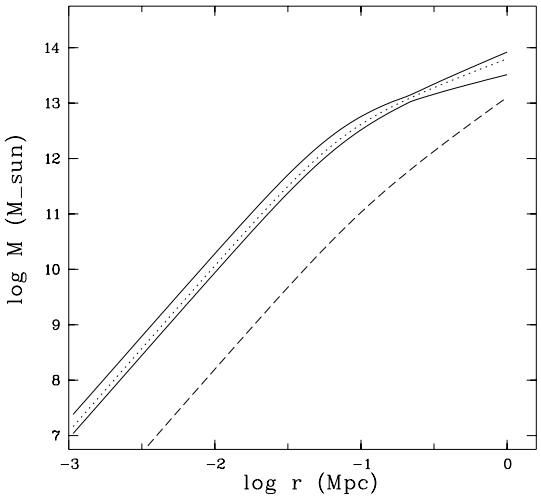

Fig. 3. Radial mass profile for the NGC 383 group of galaxies. The dashed line gives the profile of gas mass as obtained from the best-fit β-modell, the solid lines correspond to the profile of the total mass as described in the text, and the dotted line corresponds to the isothermal case.

and to systematic exclusion of individual bins (e.g., the inner or outer ones) before fitting the surface brightness profile. Our best fit leads to a larger ratio of gas to total mass at large radii. It also has consequences when comparing the pressure of the IGM with the non-thermal pressure of the radio jet (Sect. 5.1.3).

3.3. Mass determination

For the beta-modell applied in the previous section, the gas density distribution is given by

$$n_{\rm gas} = n_0 (1 + \frac{r^2}{r_{\rm c}^2})^{-\frac{3}{2}\beta} \; . \qquad (2)$$

This implies a central density n_0 = 1.3 10^{-3} cm^{-3} and a gas mass within 1 Mpc of $M_{\rm gas}$ = 1.3 10^{13} M$_\odot$.

Assuming spherical symmetry and the group to be approximately in hydrostatic equilibrium, the total gravitating mass follows the relation

$$M_{\rm total}(r) = -\frac{k}{\mu m_{\rm p} G} T(r)\, r\, (\frac{r}{T}\frac{dT}{dr} + \frac{r}{\rho}\frac{d\rho}{dr}) \; . \qquad (3)$$

With the observed parameters this results in an integrated total mass of $M_{\rm total}$ = 6.3 10^{13} M$_\odot$ within 1 Mpc radius and a gas mass fraction of 21%. Using instead the galaxy velocity dispersion as derived from optical observations, σ = 466 km/s (Ledlow et al. 1996; see also Sakai et al. 1994), and a core radius of 73 kpc we get a mass of $\sim$7 10^{13} M$_\odot$ within 1 Mpc, which is well consistent with the value obtained purely from the X-ray data.

The profile of total and gas mass is displayed in Fig. 3. Errors on the mass $M_{\rm total}$ are obtained from the temperature range allowed by the X-ray spectral analysis, kT = 1.5$\pm$0.2 keV, and a temperature profile for a family of γ models with polytropic index γ in the range 0.9–1.3. In the polytropic models the nominal temperature is fixed at the core radius.

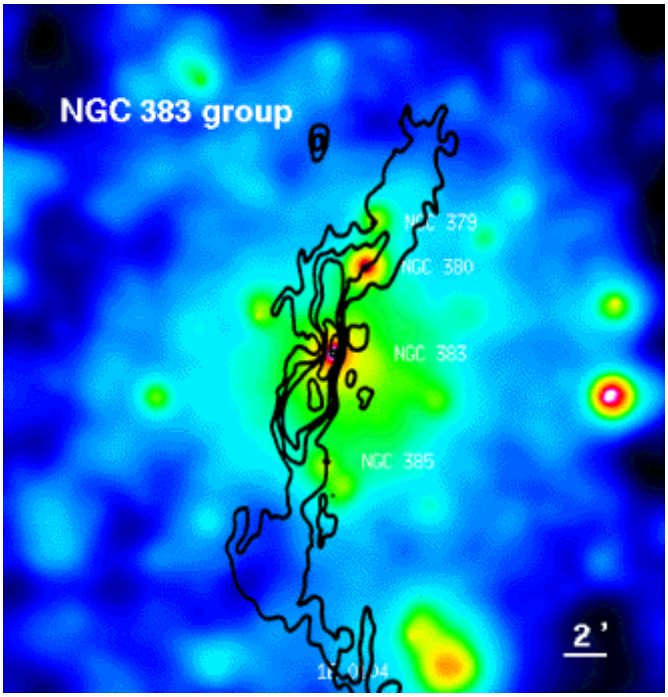

Fig. 4. Same as Fig. 1, but with overlay of the radio jet contours (Strom et al. 1983, 0.6 GHz map) on the X-ray image.

3.4. Radio – X-ray morphology

There are some spectacular examples of pressure interaction between the radio and X-ray gas in clusters of galaxies (e.g., Böhringer et al. 1993, 1995, Harris et al. 1994, Clarke et al. 1997, Otani et al. 1998). In the present case, we do not find conspicuous morphological correlations between radio- and X-ray emission (Fig. 4). This may be partly due to the narrowness of the jet, the still limited spatial resolution of the *ROSAT* PSPC, and the 2D view of the 3D source structure.

Changes of the jet orientation angle near the locations of some optical chain galaxies, now also detected as strong X-ray sources, were already noted by Strom et al. (1983).

4. Individual sources

4.1. NGC 383 = 3C 31

4.1.1. Spectral analysis

As background we chose (i) a source-free ring around the target source, and (ii) a source-free circular region near the target source. This allows to check for sensitivity against the background correction. All majour fits were repeated for both background geometries. Further, we note that the source emission in the first bin (below 0.4 keV) is weak. We repeated all fits after having removed the first bin from the spectrum. In all cases, the results presented below are found to be robust.

First, several single component models were fit to the X-ray spectrum, starting with a powerlaw (pl). Although this model fits the X-ray spectrum ($\chi^2_{\rm red}$ = 1.3), the derived parameters are unusual. The slope is extremely steep $\Gamma_{\rm x} \simeq$ –5, and there is

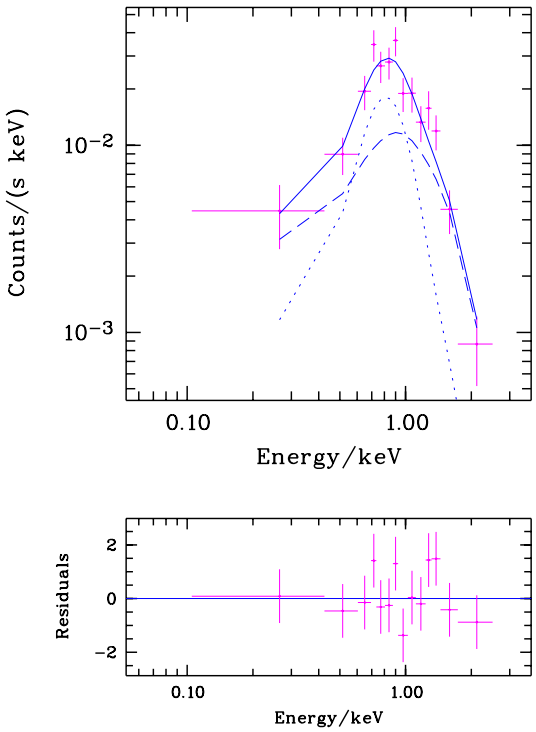

Fig. 5. The first panel shows the observed X-ray spectrum of NGC 383 (crosses) and the best-fit rs+pl model (solid line). The second panel displays the residuals for this model.

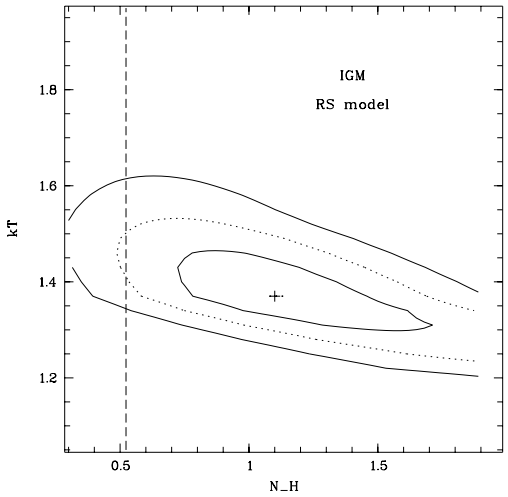

Fig. 6. Error contours in kT (in units of keV), $N_{\rm H}$ (in 10^{21} cm^{-2}) for the rs model of the IGM of the NGC 383 group. The contours are shown for confidence levels of 68.3, 95.5 and 99.7%. The dashed line marks the Galactic absorbing column density towards the X-ray center of the group.

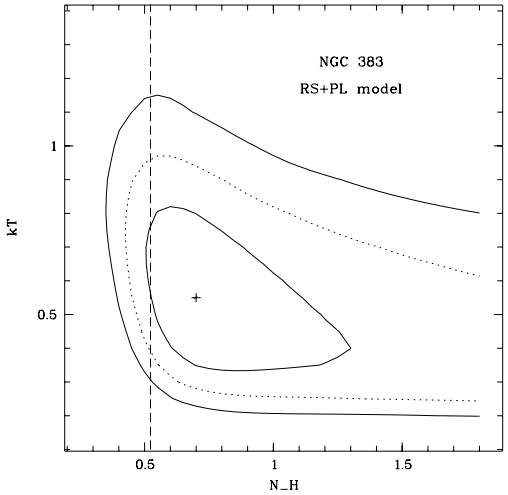

Fig. 7. Error contours in kT (in keV), $N_{\rm H}$ (in 10^{21} cm^{-2}) for the rs+pl description of NGC 383; the normalizations of the two components were free parameters, the pl index was fixed to –1.9. The contours are shown for confidence levels of 68.3, 95.5 and 99.7%. The dashed line marks the Galactic $N_{\rm H}$ towards NGC 383.

evidence for strong excess absorption (about 8 times the Galactic value). A single steep pl may be mimicked by a flat pl plus soft excess. Parameterizing the excess as black body and fixing $\Gamma_{\rm x}$=–1.9, we do not find a successful fit. This also holds for a single pl in which absorption is fixed to the Galactic value ($\chi^2{}_{\rm red}$ = 3.3). A single rs model with metal abundances of 0.35 × solar does not give an acceptable fit, either ($\chi^2{}_{\rm red}$ = 2.4). Lowering the abundances up to $\lesssim$ 0.1 × solar yields an acceptable fit (see also T97), but such low abundances are unexpected for dominant group galaxies[1].

In a second step, two-component models consisting of contributions from both, a rs plasma and a pl source, or two rs sources were applied. In the rs+pl description, the pl index was fixed to $\Gamma_{\rm x}$=–1.9 (the value typically observed in Sy; since we want to specifically test for the presence of an AGN). This provides a good fit ($\chi^2{}_{\rm red}$ = 1.1). If $N_{\rm H}$ is treated as additional free parameter, it is found to be of the order of the Galactic value. For the rs component, we obtain $kT \simeq 0.6$ keV (error contours are displayed in Fig. 7). The pl component contributes with a (0.1–2.4 keV) luminosity of $L_{\rm x,pl} = 3.5\,10^{41}$ erg/s, the total (0.1–2.4 keV) luminosity is $L_{\rm x} = 4.7\,10^{41}$ erg/s (for $N_{\rm H}$ fixed to $N_{\rm gal}$). Alternatively, the spectrum can be fit with a double rs model. In this case we find the hotter component to be ill-constrained. If we fix kT_2 = 1.5 keV, we get kT_1 = 0.4±0.2 keV ($\chi^2{}_{\rm red}$ = 1.1; we used $N_{\rm H} = N_{\rm gal}$) and luminosities of $L_{\rm x,T_1} = 1.7\,10^{41}$ erg/s, $L_{\rm x,T_2} = 2.9\,10^{41}$ erg/s. For comparison, if kT_2 = 5 keV is chosen, kT_1 = 0.5±0.2 keV ($\chi^2{}_{\rm red}$ = 1.0) and $L_{\rm x,T_1} = 2.0\,10^{41}$ erg/s, $L_{\rm x,T_2} = 2.7\,10^{41}$ erg/s. The results of the spectral fits are summarized in Table 1.

[1] E.g., Fabbiano et al. (1994) find that assuming typical stellar mass loss rates, originally primordial gas would be 10% metal-enriched after 10^7 yr; see also Sarazin (1997). For a recent thorough discussion of the issue of single-T models of very subsolar abundances vs. two-component models of ∼solar abundances see also Buote & Fabian (1998).

4.1.2. Spatial analysis

The X-ray emission from the direction of NGC 383 is strongly peaked. To check how much of the emission might arise from

Table 1. Spectral fits to individual galaxies of the group (NGC 383, NGC 380 and NGC 379) and the intra-group medium (IGM) emission (pl = power law, rs = Raymond-Smith model). T = temperature of rs component, $N_{\rm H}$ = cold absorbing column, Z = metal abundances, relative to solar (Anders & Grevesse 1989), d.o.f. = degrees of freedom. The error contours for the rs+pl model of NGC 383, and the rs model of the total IGM emission, are displayed in Figs. 7 and 6, respectively.

	model	$N_{\rm H}$ 10^{21} cm^{-2}	$\Gamma_{\rm x}$	kT keV	Z x solar	$\chi^2_{\rm red}(d.o.f)$
NGC 383	pl	4.4	-5.1	–	–	1.38 (11)
	pl	0.523[2]	-1.9	–	–	3.25 (12)
	rs	0.43	–	1.14	0.35[3]	2.42 (11)
	rs	0.59	–	0.98	0.10[3]	1.50 (11)
	rs+pl	0.69	-1.9[3]	0.55	0.35[3]	1.12 (10)
	rs+pl	0.523[2]	-1.9[3]	0.67	0.35[3]	1.18 (11)
	rs+rs	0.523[2]	–	0.5/5[5]	0.35[3]	1.02 (11)
	rs+rs	0.523[2]	–	0.4/5[5]	1.00[3]	1.01 (11)
NGC 380	pl	0.523[2]	-1.8	–	–	5.58 (7)
	rs	0.523[2]	–	0.92 ± 0.11	0.35[3]	0.84 (7)
NGC 379	pl	0.523[2]	-2.2	–	–	3.38 (4)
	rs	0.523[2]	–	0.50 ± 0.27	0.35[3]	1.03 (4)
IGM	rs; total	0.523[2]	–	1.46 ± 0.08	0.35[3]	1.14 (22)
	rs; total	0.523[2]	–	1.56 ± 0.12	1.00[3]	0.73 (22)
	rs; inn.	0.523[2]	–	1.48 ± 0.12	0.35[3]	1.43 (18)
	rs; mid.	0.523[2]	–	1.56 ± 0.17	0.35[3]	1.79 (19)
	rs; out.	0.523[2]	–	1.37 ± 0.14	0.35[3]	1.42 (14)

[2] fixed to the Galactic value; [3] fixed; [5] temperature of second rs component, fixed

a point source we compared the radial source profile with the instrumental point-spread function (PSF). We find that the emission from NGC 383 is not significantly extended beyond the PSF of the PSPC. Thus, the data are consistent with the bulk of the X-ray emission arising from a point source.

Performing a similar analysis for the HRI observation, we find a deviation of the source profile from the HRI PSF. However, similar deviations are found for the (presumably pointlike) F star which is located within the field of view (after taking into account the appropriate off-axis PSF for the star). We conclude that in the present data there is no evidence for source extent.

4.1.3. Temporal analysis

The X-ray lightcurve of NGC 383 is displayed in Fig. 8. An AGN/point-source might reveal itself by variability (but not necessarily). We find a constant source flux within the errors.

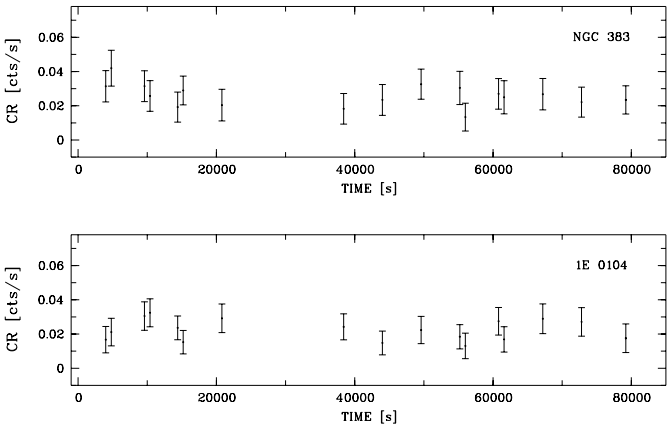

Fig. 8. PSPC X-ray lightcurve of NGC 383 (upper panel) and 1E 0104 (lower panel) binned to time intervals of 800 s. The time is measured in seconds from the start of the observation.

4.2. NGC 379, NGC 380, NGC 384, NGC 385

A spectral analysis was performed for the two X-ray brightest galaxies, NGC 379 and NGC 380. A pl model does not provide an acceptable fit ($\chi^2_{\rm red}$ = 3.4 and 5.6) with residuals strongly indicative of the presence of an rs component. Such a model indeed gives an excellent fit ($\chi^2_{\rm red}$ = 1.0 and 0.8). We find temperatures of 0.5 keV (NGC 379) and 0.9 keV (NGC 380). The absorption-corrected fluxes for this model description in the (0.1–2.4) keV band are $f_{\rm x} = 8.5\,10^{-14}$ erg/cm^2/s (NGC 379) and $f_{\rm x} = 1.85\,10^{-13}$ erg/cm^2/s (NGC 380), and the corresponding luminosities $L_{\rm x} = 1.1\,10^{41}$ erg/s (NGC 379) and $L_{\rm x} = 2.3\,10^{41}$ erg/s (NGC 380).

To estimate luminosities also for NGC 384 and 385, which are too weak to allow direct spectral fits, we adopted a rs spectrum of 0.5 keV. The derived luminosities are given in Table 2.

4.3. $L_{\rm x} - L_{\rm B}$ relation

To compare the derived X-ray luminosities with blue luminosities we used the observed blue magnitudes of de Vaucouleur et al. (1991 via NED; see also Smith et al. 1997). For the extinction

Table 2. Summary of the properties of the X-ray brightest group galaxies.

galaxy	CR 10^{-2} cts/s	$kT^{(1)}$ keV	$L_{(0.1-2.4)\mathrm{keV}}$ erg/s	L_{B} erg/s
NGC 379	0.58	0.5	$1.1\,10^{41}$	$3.1\,10^{43}$
NGC 380	1.24	0.9	$2.3\,10^{41}$	$4.0\,10^{43}$
NGC 383	2.40	0.6+pl	$4.7\,10^{41}$	$5.1\,10^{43}$
NGC 384	0.21	0.5*	$5.0\,10^{40}$	$1.8\,10^{43}$
NGC 385	0.41	0.5*	$7.6\,10^{40}$	$2.6\,10^{43}$

(1) either determined directly from spectral fit (Sect. 4.1.1, 4.2) or fixed to 0.5 keV (marked with '*') in cases where the spectrum could not be fit directly.

Table 3. Summary of the properties of the NGC 383 group of galaxies as derived from the X-ray analysis.

spectral fits:
kT=1.5 keV, $L_{\mathrm{x}}^{0.1-2.4\,\mathrm{keV}} = 1.5\,10^{43}$ erg/s
beta-model results:
$S_0 = 2.7\,10^{-3}$ cts/s/arcmin^2, $\beta = 0.38$, $r_{\mathrm{c}} = 73$ kpc
central density, mass:
$n_0 = 1.3\,10^{-3}$ cm^{-3}; $M_{\mathrm{total}} = 0.6\,10^{14}$ M$_\odot$,
gas mass fraction 21% (at r = 1 Mpc)

correction we converted the Galactic N_{H} as given in Dickey & Lockman (1990) into A_{B} assuming a standard gas/dust ratio, the relation of Bohlin et al. (1978; see also Predehl & Schmitt 1995), and the extinction curve as given in Osterbrock (1989, his Table 7.2). This yields $A_{\mathrm{B}} = 0.38^{\mathrm{m}}$. L_{B} was then calculated using $L_{\mathrm{B}} = 4\pi d^2 10^{(-0.4 m_{\mathrm{B}} - 5.19)}$ and assuming the same z=0.017 for all galaxies. Results are listed in Table 2.

5. Discussion

5.1. The group

5.1.1. IGM

The NGC 383 group turns out to be the brightest group in X-ray luminosity when compared to the samples of Ponman et al. (1996) and Mulchaey & Zabludoff (1998).

How does it fit into the known $L_{\mathrm{x}} - T$ relation for groups and clusters of galaxies (e.g., Fabian et al. 1994, White 1996, Ponman et al. 1996, Arnaud & Evrard 1998, Reiprich 1998)? Since T is outside the range for which Ponman et al. find a very steep $L_{\mathrm{x}} - T$ dependence, we use the relation of Markevitch (1998) which predicts a (0.1–2.4 keV) X-ray luminosity $L_{\mathrm{x}} \simeq 3\,10^{43}$ erg/s. This agrees well with the observed value of $1.5\,10^{43}$ erg/s.

For the given kT = 1.5 keV, and a galaxy velocity dispersion of σ = 466 km/s (Ledlow et al. 1996; see also Sakai et al. 1994) we derive $\beta_{\mathrm{spec}} = \frac{\mu m_{\mathrm{p}} \sigma_{\mathrm{r}}^2}{kT} = 0.95$.

The low value of the slope parameter β derived from the X-ray spatial analysis is in line with earlier findings of a trend of decreasing β toward lower T (e.g., David et al. 1990, White 1991, Arnaud & Evrard 1998) which is reproduced by models of cluster formation that incorporate galactic winds (e.g., Metzler & Evrard 1997).

Assuming spherical symmetry and isothermality, the total gravitating mass within 1 Mpc amounts to $M_{\mathrm{total}} = 0.6\,10^{14}$ M$_\odot$. We find a gas mass fraction of 21% which is at the upper end of the values typically observed in groups (3–25%, e.g., David et al. 1995, Böhringer 1995) but not inconsistent with similar results for such X-ray luminous groups as for example NGC 533 or NGC 4104 (Mulchaey et al. 1996). The gas mass fraction slightly decreases with decreasing radius.

Concerning the morphology of the IGM, we note that the rather spherically symmetric shape of the extended emission, as compared to the completely different morphology defined by the bright ellipticals aligned in a chain, argues against an origin of the gas in terms of halos of the chain galaxies, but rather for an association with the global group potential.

The X-ray emission of the IGM can be traced out to about 1 Mpc, which turns out to be about the virial radius of the group if we use the total mass value determined from the X-ray observations and the assumption that the virial radius is approximately characterized by the region inside which the mean overdensity is a factor of 200 above the critical density of the universe (e.g., Evrard et al. 1996).

The fairly spherically symmetric appearance of the group's X-ray halo (except possibly for some faint outer extensions) taken together with the perfect consistency of the mass determined from the velocity dispersion and the X-ray properties, and the findings of Ledlow et al. (1996) that the galaxy velocity distribution does not significantly deviate from a Gaussian, implies that the matter in the group inside a radius of about 1 Mpc is most probably quite relaxed.

The position of the central galaxy NGC 383 is found to be slightly off-set from the center of the extended X-ray emission, and thus presumably from the center of the dark matter potential. Such off-sets of cD galaxies have also been observed in a number of other poor systems (e.g., AWM 7, Neumann & Böhringer 1995; Fornax cluster, Ikebe et al. 1996) and some Abell clusters (e.g., Lazzati & Chincarini 1998). In Lazzati & Chincarini (1998), this is traced back to a small-amplitude oscillation of the cD galaxy around the bottom of the cluster potential.

5.1.2. Presence of a cooling flow?

The cooling time in the center is $t \simeq 2.7\,10^{10}$ yr, i.e. no 'large-scale' cooling flow is expected to have developed. Further, the enhanced X-ray emission from the direction of NGC 383 is consistent with originating from a point source.

We also note that although strong low-ionization optical emission lines have been reported for some central galaxies in cluster cooling flows (e.g., Cowie et al. 1983, Heckman 1989, Crawford & Fabian 1992), the morphology of the ring- or disk-like emission line region in NGC 383 (Owen et al. 1990, Fraix-Burnet et al. 1991) does not argue for a connection to a cooling flow. Further, we find the locus of NGC 383 in the emission

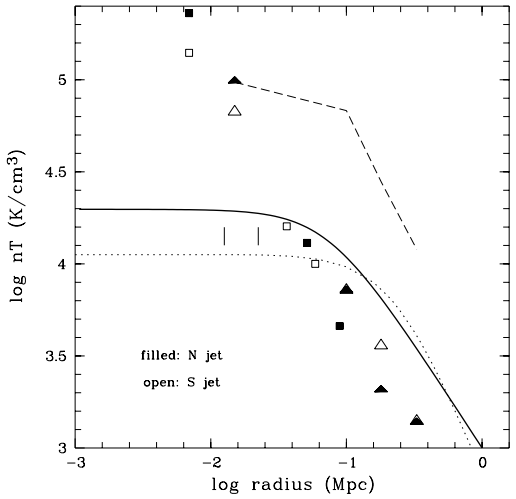

Fig. 9. Comparison of different pressure estimates. The solid line gives the thermal pressure as derived from the present *ROSAT* X-ray observation. The symbols mark the non-thermal pressure as given in Strom et al. (1983; squares) and Morganti et al. (1988, triangles); the filled symbols are for the northern jet, the open ones for the southern jet. The vertical bars mark a scale of 25″ (left) and the optical extent of NGC 383 (as given in NED; right). Also drawn is the change in thermal pressure according to two previous estimates (dashed line: Morganti et al. 1988; dotted: T97).

line-ratio diagram [SII] vs. [NII] to ly outside of the 'class I' and 'class II' cooling flow nebulae of Heckman et al. (1989; see their Fig. 6). (This alone does not exclude the presence of a cooling flow, though, since not all of them are associated with emission line nebulae.)

5.1.3. Radio - X - relations, pressure estimate

Although 3C 31 is only a moderately bright radio galaxy, its jets could be studied in detail due to its proximity. Concerning the origin, morphology and confinement of the jets, several models were explored (e.g., Blandford & Icke 1978, Bridle et al. 1980, Bicknell 1984).

The gas density and temperature derived for the X-ray gas allow a comparison with the pressure of the radio gas, and an assessment of the confinement of the jet material. In Fig. 9 we compare the pressure of the radio emitting region as given in Strom et al. (1983) and Morganti et al. (1988)[2] with the thermal pressure of the X-ray gas derived from the run of density (Sect. 3.3) and a temperature of kT=1.5 keV. Whereas in the central region (i.e. within NGC 383), there seems to be a strong overpressure of the radio gas (but note that there certainly is an additional contribution to thermal pressure from higher-density gas within the galaxy), pressure equilibrium is reached at about 35 kpc (projected distance from the center). Further out the thermal pressure increasingly exceeds the nonthermal pressure.

It is interesting to note that Bridle et al. (1980) find the expansion rate of the jets of 3C 31 transverse to their length to decrease with increasing distance from the radio core. This may be related to the relative increase of the thermal pressure of the ambient medium with increasing radius. While Bridle's trend refers mainly to the presently in X-rays barely resolved core region it may be interesting to explore this relation further with higher-resolution X-ray data.

A similar comparison of thermal vs. non-thermal pressure was performed in T97. They derived a somewhat different surface brightness profile and thus change in thermal pressure with the consequence that the radius where both pressure values are of the same order shifts further out which led them to suggest that NGC 383 might have a giant halo that escaped detection in the (short) HRI exposure.

5.2. *Individual sources*

5.2.1. $L_{\rm X} - L_{\rm B}$ relation

The galaxies of the chain are among those with high $L_{\rm x}/L_{\rm B}$ and show a larger spread in $L_{\rm x}$ than in $L_{\rm B}$ as often observed (e.g., Eskridge et al. 1995).

The high $L_{\rm x}$ in cluster/group ellipticals (e.g., Fig. 1 of Brown & Bregman 1998, Fig. 2 of Beuing et al. 1998, Fig. 1 of Irwin & Sarazin 1998) are usually traced back to the influence of the surroundings, via accretion of gas from the group environment (e.g., Beuing et al. 1998), or stiffling of winds by the ambient medium (Brown & Bregman 1998); see also Mathews & Brighenti (1998). The low $L_{\rm X}/L_{\rm B}$ systems seem to be dominated by discrete sources, mainly LMXBs (e.g., Canizares et al. 1987, Irwin & Sarazin 1998).

The present galaxies show a wide range in $L_{\rm x}$ reaching up to the high end of the $L_{\rm x}/L_{\rm B}$ relation. (Fig. 10; note that the objects of very high $L_{\rm x}$ of the sample of Beuing et al. 1998 are all ellipticals in the *cluster* environment). The X-ray luminosities generally exceed those expected from a discrete source contribution and the X-ray properties of most galaxies are consistent with the bulk of the X-ray emission arising from the ISM of the individual galaxies. NGC 383 is separately discussed in the next section.

5.2.2. NGC 383

The X-ray analysis suggests the presence of two components in the X-ray spectrum of NGC 383: emission from a rs plasma of $kT \simeq$ 0.4–0.7 keV and a second component that was parameterized as powerlaw or second rs contribution.

Compact pl emission could originate from an AGN or via SSC at the base of the radio jet; e.g., Jones et al. (1974), Marscher (1987), Birkinshaw & Worrall (1993). Using the correlation of 1 keV X-ray core flux with 5 GHz radio core flux of Worrall et al. (1994, their Fig. 3; see also Fabbiano et al. 1984) we find 3C 31 above this relation (a factor ∼6 in X-ray flux for the given radio

[2] To derive the equipartition pressure, they used the equations of Pacholczyk (1970) and made the standard assumptions of equal energy density in protons and electrons, filling factor of 1, and a powerlaw representation of the radio spectrum with cut-offs at 10 MHz and 100 GHz.

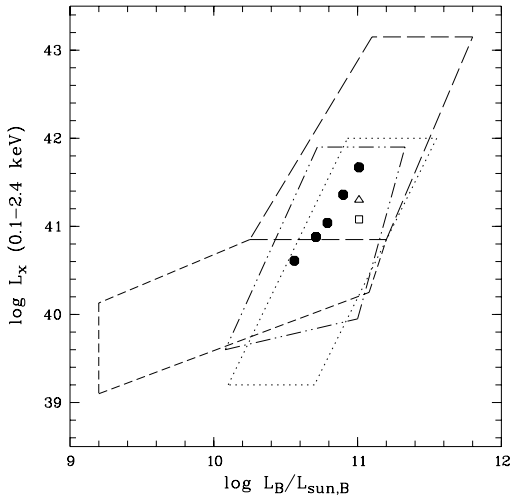

Fig. 10. Locations of the chain galaxies in the $L_{\rm x} - L_{\rm B}$ diagram (fat circles; NGC 383, NGC 380, NGC 379, NGC 385, NGC 384 from top to bottom; see also T97). For comparison, we sketch the regions populated by some larger samples of ellipticals (note that these $L_{\rm x}$ were derived under slightly different assumptions, i.e. source extraction radii and energy bands which we did not correct for since we only intend to show the rough trends). Dotted: Brown & Bregman 1998, dot-dashed: Canizares et al. 1987, long-dashed: Beuing et al. 1998 (detections), short-dashed: Beuing et al. 1998 (upper limits). The open square (triangle) marks the locus of NGC 383 after subtraction of the contribution of the pl (hot rs) component to $L_{\rm x}$.

core flux[3]), and within the region populated by lobe-dominated quasars.

Is there evidence for a relatively *unobscured* view on an AGN? Optical emission line ratios were presented by Owen et al. (1990), who found the line ratios in the disk to be similar to those at the nucleus ([NII]/Hα=1.5, [SII]/Hα=0.5, [OIII]/Hα=0.1) and concluded that the disk ionization is probably driven by the nucleus. Plotting these line ratios in the diagnostic diagrams of Veilleux & Osterbrock (1987) we find them to be LINER-like. The dominant excitation mechanism in LINERS is still under discussion, but there is growing evidence that the bulk of them is accretion-powered (e.g., Ho 1998). Owen et al. also briefly mention the presence of a broad emission line component.

Alternatively, two-component rs models fit the X-ray spectrum; a second component may originate from non-perfect correction of the cluster contribution or a temperature range in emission from the ISM of the galaxy. In fact, more than one temperature component is favoured for nearly every early-type galaxy examined in, e.g., Matsushita et al. (1994), Matsumoto et al. (1997) and Buote & Fabian (1998). Whereas the hot component is occasionally interpreted in terms of emission from discrete sources (e.g., Matsushita et al. 1994), we find its luminosity ($L_{\rm x,pl} = 3.5\,10^{41}$ erg/s, $L_{\rm x,rs} \simeq 3\,10^{41}$ erg/s if parameterized by a pl or rs model, respectively) to be higher than expected from discrete sources (e.g., Canizares et al. 1987) for the given $L_{\rm B}$.

In conclusion, although the exact shape and strength of the hard X-ray component cannot be determined with present data, its presence and high luminosity suggest as origin emission from an active nucleus in NGC 383.

[3] we used the 5 GHz core radio flux as given in Lara et al. (1997), 90 mJy, and the rs+pl X-ray spectral model with $N_{\rm H} = N_{\rm Gal}$ for which we derive a 1 keV X-ray flux in the pl component of 0.058 μJy

6. 1E 0104+3153 (z=2 BAL quasar/ elliptical/ IGM of group)

The source 1E 0104 was serendipitously detected as bright X-ray emitter by *Einstein* and was found to be close to a BAL quasar with z=2.027 (Stocke et al. 1984). Since the QSO is also located very near (10″) to a giant elliptical galaxy at z=0.111, which is part of a small group, it remained unclear from which of the three the X-ray emission originated: the QSO, the giant elliptical, or the IGM of the small group (Stocke et al. 1984). Gioia et al. (1986), in a deep *EXOSAT* observation, could not detect X-ray emission in the 0.05–2 keV band, which they traced back to either variability (intrinsic to the source, or caused by a microlensing event during the *Einstein* observation; which would favour the quasar identification of the X-ray source), or a strongly absorbed X-ray spectrum. The incidental *ROSAT* PSPC observation of the source was briefly discussed by Ciliegi & Maccacaro (1996) in a large sample study of *ROSAT* spectra of EMSS AGN. They applied a powerlaw to the spectrum and found excess absorption.

Below, we analyze the X-ray spectral properties in more detail and also perform a timing analysis, in order to get clues on the origin of the X-ray emission (elliptical galaxy, group or quasar).

6.1. Data analysis

6.1.1. Spatial analysis

The HRI data improve the position of 1E 0104, but not much, since the source is weak and located near the border of the fov. In Fig. 11 we compare the *ROSAT* HRI position with the optical positions of the quasar and the galaxies (as given in Stocke et al. 1984; all coordinates were converted to J 2000) and the *Einstein* IPC position. Both sources, the quasar and the elliptical, remain within the error circle.

We note, however, that the X-ray source appears to be extended. Although the analysis is complicated by a newly detected closeby second source, a comparison with the X-ray emission from the F star at nearly the same off-axis angle, clearly suggests that the X-ray emission from 1E 0104 does not originate from a point source (see Fig. 1; the F star is the brightest source at the right border of the image, 1E 0104 is the one at the lower border).

6.1.2. Temporal analysis

We do not detect short-time variability during the PSPC observation (Fig. 8). To examine the long-term trend, we converted the PSPC countrate to HRI countrate assuming constant spec-

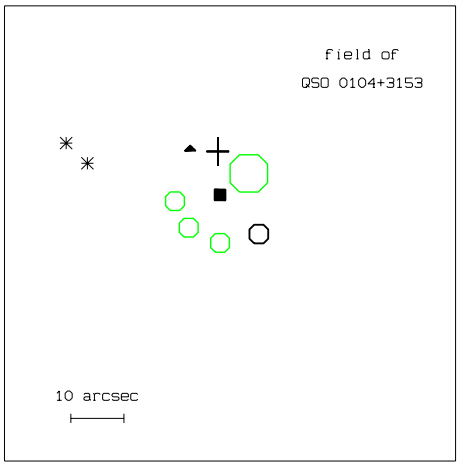

Fig. 11. Optical and X-ray positions for the field around QSO 0104 and the nearby elliptical galaxy. The circles and asterisks correspond to optical positions derived by Stocke et al. (1984; large circle: giant elliptical, small fat circle: QSO 0104, further circles: galaxies, members of a small group, asterisks: stars). The filled symbols and the cross mark X-ray positions measured by different instruments (cross: *Einstein* IPC, filled triangle: *ROSAT* PSPC, filled square: *ROSAT* HRI).

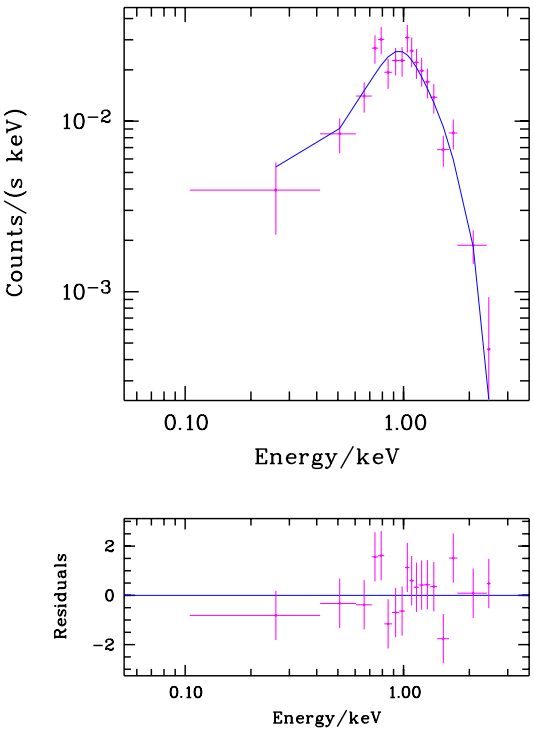

Fig. 12. Observed (crosses) and fit (solid line) X-ray spectrum (upper panel) and residuals (lower panel) for the Raymond-Smith model fit to 1E 0104.

tral shape. Again, the source emission is found to be constant. We then compared with the *Einstein* IPC flux (this obs. was performed 11 yrs prior to the *ROSAT* PSPC observation) given in Stocke et al. (1984). To this end, we first re-fit the *ROSAT* data with the same spectral model as in Stocke et al. (they used $\Gamma_{\rm x}$=–1.5 and $N_{\rm H} = 0.3\,10^{20}$ cm^{-2}; see Gioia et al. 1986 for similar parameters). We then derive an observed flux (converted to the 0.3–3.5 keV band) of $f_{\rm ros} = 3.96\,10^{-13}$ erg/cm^2/s which is in excellent agreement with the *Einstein* flux of $f_{\rm ein} = 4.0(\pm0.7)\,10^{-13}$ erg/cm^2/s.

6.1.3. Spectral analysis

A powerlaw with absorption fixed to the Galactic value does not give a good fit with $\Gamma_{\rm x}$= –1.7 and $\chi^2_{\rm red}$ = 1.5. The fit improves after allowing for excess cold absorption. This yields $N_{\rm H} = 2.9\,10^{21}$ cm^{-2}, $\Gamma_{\rm x}$= –3.2 and $\chi^2_{\rm red}$ = 1.1. Alternatively, the spectrum can be successfully described in terms of a rs model. In this case we used z=0.111 since rs emission is more likely to originate from the elliptical and/or IGM. If $N_{\rm H}$ is treated as free parameter it is consistent with $N_{\rm gal}$ but comes with large errors. We obtain $N_{\rm H} = (0.66^{+0.34}_{-0.16})\,10^{21}$ cm^{-2} and $kT = 1.89^{+1.11}_{-0.29}$ keV ($\chi^2_{\rm red}$ = 1.0). For $N_{\rm H}$=$N_{\rm gal}$, kT = 1.9 keV and $L_{\rm x} = 3\,10^{43}$ erg/s.

Plugging this temperature into the $L_{\rm x} - T$ relation for groups/clusters (Markevitch 1998) we predict a (0.1–2.4 keV) X-ray luminosity of $5\,10^{43}$ erg/s which is of the order of the observed value and thus consistent with an identification of 1E 0104 with the IGM of the small group.

6.1.4. Discussion

The X-ray emission of 1E 0104 turned out to be constant. In particular, there is excellent agreement with the flux derived for the *Einstein* observation (adopting the same spectral model). This renders one of several possibilities discussed in Stocke et al. (1984) – the one that the quasar was temporarily brightened via microlensing during the *Einstein* observation – unlikely.

We confirm the excess cold absorption in case of the pl description of the X-ray spectrum, not unexpected for a BAL quasar, but find an rs model to be similarly successful. The best-fit parameters of the latter model, which due to its shape would argue for an origin from the group's IGM or brightest group elliptical, are well consistent with the known $L_{\rm x}$-T relation of clusters and groups of galaxies, i.e., with the IGM as counterpart. Further, the derived $L_{\rm x} \simeq 3\,10^{43}$ erg/s would be rather high for an elliptical outside a rich cluster environment (particularly for the observed (Stocke et al. 1984) R-magnitude of $m_{\rm R}$ = 15.1), but usual for the IGM. The HRI position is intermediate between the elliptical and the quasar, and consistent with all three identifications. However, there is evidence that the source emission is extended.

In summary, if only one emitter dominates the X-ray flux (instead of a contribution from *all three* potential counterparts, which would strongly complicate matters but cannot be excluded) it seems that the available data (constancy in source flux, high $L_{\rm x}$, fit into $L_{\rm x}$-T relation, evidence for source extent) favour an identification with the IGM of the nearby group at z=0.111. A deep high spatial resolution observation *centered* on 1E 0104 should finally resolve the counterpart question.

7. Summarizing conclusions

We have presented a study of the X-ray properties of the NGC 383 group of galaxies, extending the work of T97, and of the source 1E 0104+3135.

The properties of the intra-group medium derived from the *ROSAT* PSPC observation are summarized in Table 3. The X-ray emission of the IGM can be traced out to about $1h_{50}^{-1}$ Mpc, which turns out to be about the virial radius of the group. Several lines of evidence were presented that the group inside this radius is quite relaxed. With the given depth of the *ROSAT* PSPC observations we can therefore characterize the entire galaxy system as far as it has approached a dynamical equilibrium state. For this part of the group we find a total mass of $6\,10^{13}h_{50}^{-1}$ $M_\odot$ and a gas mass fraction of 21%. The latter value is at the upper end of the distribution for groups. The result implies that the gravitational potential of the group is deep enough to prevent a majour gas loss, in contrast to less massive groups (Davis et al. 1998).

The surface brightness profile is characterized by a slope parameter $\beta \simeq 0.4$ which is shallower than for most of the galaxy clusters but a quite common value for groups. The temperature of 1.5 keV found for the IGM is well consistent with the $L_x - T$ relation giving further support to the picture that the group is a well relaxed and normal system.

With an estimated central cooling time larger than the Hubble time no central cooling flow is expected and no signature for it is found neither in the spatial and spectral X-ray data nor in the optical spectrum.

We do not find any conspicuous spatial correlation of X-ray emission and radio jet which might be partly due to the narrowness of the jet and the 2D view of the 3D source structure.

We also discussed the X-ray properties of the well-studied radio galaxy 3C 31 which is located near the center of the extended X-ray emission. If one wishes to avoid excessively depleted metal abundances, the spectrum of 3C 31 is best described by a two-component model, consisting of a low-temperature rs component and a hard tail (pl or second rs), confirming T97. The soft component contributes with $\simeq 3\,10^{41}$ erg/s to the total X-ray luminosity of $L_{\rm x} \simeq 5\,10^{41}$ erg/s (assuming metal abundances of 0.35$\times$solar). No temporal variability in the X-ray flux is detected.

X-ray emission from the direction of the interesting source 1E 0104+3135, by chance located in the field of view, was analyzed. One scenario (transient brightening of the z=2 BAL QSO 0104+3135 due to lensing during the earlier *Einstein* observation) turned out to be unlikely. Besides an absorbed powerlaw, the spectrum of 1E 0104 can be described by a Raymond-Smith model with $kT \simeq 2$ keV resulting in an intrinsic luminosity of $L_{\rm x} \simeq 3\,10^{43}$ erg/s at z=0.111. Although no potential counterpart (QSO, nearby elliptical galaxy or IGM of the small group to which the elliptical belongs) can be safely ruled out at present, there are several hints (constancy in source flux, high $L_{\rm x}$, consistency with $L_{\rm x}$-T relation for groups/clusters, evidence for source extent) for an identification of the X-ray source with the IGM of the nearby group of galaxies at z=0.111.

Acknowledgements. We acknowledge support from the Verbundforschung under grant No. 50 OR 93065. It is a pleasure to thank Vadim Burwitz for help with Fig. 4. The *ROSAT* project is supported by the German Bundesministerium für Bildung, Wissenschaft, Forschung und Technologie (BMBF/DLR) and the Max-Planck-Society. This research has made use of the NASA/IPAC extragalactic database (NED) which is operated by the Jet Propulsion Laboratory, Caltech, under contract with the National Aeronautics and Space Administration.

References

Andernach H., Ferretti L., Giovannini G., et al., 1992, A&AS 93, 331
Anders E., Grevesse N., 1989, Geochimica & Cosmochimica Acta 53, 197
Arnaud M., Evrard A.E., 1998, astro-ph/9806353
Arp H., 1966, Atlas of peculiar galaxies. Cal. Inst. of Techn., Pasadena
Arp H., 1968, PASP 80, 129
Arp H., Bertola F., 1971, ApJ 163, 195
Artyukh V.S., Ogannisyan M.A., Tyul'bashev C.A., 1994, Astr. Let. 20, 211 (= Pis'ma Astr. Zh. 20, 258)
Beuing J., Döbereiner S., Böhringer H., Bender R., 1998, submitted to MNRAS
Bicknell G.V., 1984, ApJ 286, 68
Birkinshaw M., Worrall D.M., 1993, ApJ 412, 568
Blandford R.D., Icke V., 1978, MNRAS 185, 527
Böhringer H., 1995, In: Böhringer H., Morfill G.E., Trümper J. (eds.) 17th Texas Symp. on Relativistic Astrophys. and Cosmology, Ann.N.Y.Acad.Sc. 759, 67
Böhringer H., Voges W., Fabian A.C., Edge A.C., Neumann D.M., 1993, MNRAS 264, L25
Böhringer H., Nulsen P.E.J., Braun R., Fabian A.C., 1995, MNRAS 274, L67
Böhringer H., Tanaka Y., Mushotzky R.F., Ikebe Y., Hattori M., 1998, A&A 334, 789
Bohlin R.C., Savage B.D., Drake J.F., 1978, ApJ 224, 132
Bridle A.H., Henriksen R.N., Chan K.L., et al., 1980, ApJ 241, L145
Brown B.A., Bregman J.N., 1998, ApJ 495, L75
Buote D.A., Fabian A.C., 1998, MNRAS 296, 977
Burch S.F., 1977, MNRAS 181, 599
Burch S.F., 1979, MNRAS 187, 187
Butcher H.R., van Breugel W., Miley G.K., 1980, ApJ 235, 749
Canizares C.R., Fabbiano G., Trinchieri G., 1987, ApJ 312, 503
Cavaliere A., Fusco-Femiano R., 1976, A&A 49, L137
Ciliegi P., Maccacaro T., 1996, MNRAS 282, 477
Clarke D.A., Harris D.E., Carilli C.L., 1997, MNRAS 284, 981
Condon J.J., Frayer D.T., Broderick J.J., 1991, AJ 101, 362
Cowie L.L., Hu E.M., Jenkins E.B., York D.G., 1983, ApJ 272, 29
Crawford C.S., Fabian A.C., 1992, 259, 265
David L.P., Arnaud K.A., Forman W., Jones C., 1990, ApJ 356, 32
David L.P., Jones C., Forman W., 1995, ApJ 445, 578
Davis D.S., Mulchaey J.S., Mushotzky R.F., 1998, ApJ in press, astro-ph/9808085
de Vaucouleurs G., de Vaucouleurs A., Corwin J.R., et al., 1991, Third reference catalogue of bright galaxies. Springer, New York
Dickey J.M., Lockman F.J., 1990, ARA&A, 28, 215
Ekers R.D., Fanti R., Lari C., Parma P., 1981, A&A 101,194
Eskridge P.B., Fabbiano G., Kim D.-W., 1995, ApJS 97, 141
Evrard A.E., Metzler C.A., Navarro J.N., 1996, ApJ, 469, 494
Fabian A.C., Crawford C.S., Edge A.C., Mushotzky R.F., 1994, MNRAS 267, 779

Fabbiano G., Miller L., Trinchieri G., Longair M., Elvis M., 1984, ApJ 277, 115
Fabbiano G., Kim D.-W., Trinchieri G., 1994, ApJ 429, 92
Fomalont E.B., Bridle A.H., Willis A.G., Perley R.A., 1980, ApJ 237, 418
Fraix-Burnet D., Golombek D., Macchetto F.D., 1991, AJ 102, 562
Garcia A.M., 1993, A&AS 100, 47
Gioia I.M., Maccacaro T., Schild R.E., Giommi P., Stocke J.T., 1986, ApJ 307, 497
Gorenstein P., Fabricant D., Topka K., Harnden F.R. Jr, Tucker W.H., 1978, ApJ 224, 718
Harris D.E., Carilli C.L., Perley R.A., 1994, Nat 367, 713
Heckman T.M., Baum S.A., van Breugel W.J.M., McCarthy P., 1989, ApJ 338, 48
Heisler J., Tremaine S., Bahcall J.N., 1985, ApJ 298, 8
Henkel C., Wang Y.P., Falcke H., Wilson A.S., Braatz J.A., 1998, A&A 335, 463
Ho L., 1998, astro-ph/9807273, to appear in: The 32nd COSPAR Meeting, Adv. Space Res.
Ikebe Y., Ezawa H., Fukazawa Y., et al., 1996, Nat 379, 427
Irwin J.A., Sarazin C.L., 1998, ApJ 499, 650
Jones C., Forman W., 1984, ApJ 276, 38
Jones T.W., O'Dell S.L., Stein W.A., 1974, ApJ 188, 353
Keel W.C., 1988, ApJ 329, 532
Klein U., Wielebinski R., 1979, A&A 72, 229
Kormendy J., Bahcall J.N., 1974, AJ 79, 671
Lara L., Cotton W.D., Feretti L., et al. 1997, ApJ 474, 179
Lazatti D., Chincarini G., 1998, A&A in press, astro-ph/9807170
Ledlow M.J., Loken C., Burns J.O., Hill J.M., White R.A., 1996, AJ 112, 388
Macdonald G.H., Kenderline S., Neville A.C., 1968, MNRAS 138, 259
Markevitch M., 1998, ApJ in press, astro-ph/9802059v2
Marscher A.P., 1987, In: Zensus A., Pearson T.J. (eds.) Superluminal Radio Sources. 280
Mathews W.G., Brighenti F., 1998, astro-ph/9806350
Matsumoto H., Koyama K., Awaki H., et al., 1997, ApJ 482, 133
Matsushita K., Makishima H., Awaki C.R., et al., 1994, ApJ 436, L41
Metzler C.A., Evrard A.E., 1997, astro-ph/9710324
Morganti R., Fanti R., Gioia I.M., et al., 1988, A&A 189, 11
Moss C., Dickens R.J., 1977, MNRAS 178, 701
Mulchaey J.S., Davis D.S., Burstein D., 1996, ApJ 456, 80
Mulchaey J.S., Zabludoff A.I., 1998, ApJ 496, 73
Neumann D.M., Böhringer H., 1995, A&A 301, 865
Osterbrock D.E., 1989, Astrophysics of Gaseous Nebulae and Active Galactic Nuclei. Univ. Sci. Books, Mill Valley
Otani C., Brinkmann W., Böhringer H., et al., 1998, A&A in press (IoA prep. A98-16)
Owen F.N., O'Dea C.P., Keel W.C., 1990, ApJ 352, 44
Pacholczyk A.G., 1970, Radio Astrophysics. Freeman & Co., San Francisco
Pfeffermann E., Briel U.G., Hippmann H., et al., 1987, SPIE 733, 519
Ponman T.J., Bourner P.D.J., Ebeling H., Böhringer H., 1996, MNRAS 283, 690
Predehl P., Schmitt J.H.M.M., 1995, A&A 293, 889
Reiprich T., 1998, Diplom thesis, LMU München
Sarazin C., 1997, In: Arnaboldi M., DaCosta G., Saha P. (eds.) The Nature of Elliptical Galaxies. ASP conf. ser. 116, 375
Sakai S., Giovanelli R., Wegner G., 1994, AJ 108, 33
Smith R.J., Lucey J.R., Hudson M.J., Steel J., 1997, MNRAS 291, 461
Stocke J.T., Liebert J., Schild R., Gioia I.M., Maccacaro T., 1984, ApJ 277, 43
Strom R.G., Fanti R., Parma P., Ekers R.D., 1983, A&A 122, 305
Trümper J., 1983, Adv. Space Res. 2, 241
Trussoni E., Massaglia S., Ferrari R., et al., 1997, A&A 327, 27 (T97)
van Breugel W., 1982, A&A 110, 225
Veilleux S., Osterbrock D.E., 1987, ApJS 63, 295
White R.E. III, 1991, ApJ 367, 69
White D.A., 1996, In: Zimmermann H.U., Trümper J., Yorke H. (eds.) Röntgenstrahlung from the Universe. MPE report 263, 621
Worrall D.M., Lawrence C.R., Pearson T.J., Readhead A.C.S., 1994, ApJ 420, L17
Zimmermann H.U., Becker W., Belloni T., et al., 1994, MPE report 257
Zwicky F., Herzog E., Wild P., Karpowicz M., Kowal C.T., 1961–68, Catalogue of Galaxies and Clusters of Galaxies. Vol. 1–6, Cal. Inst. of Techn., Pasadena